A method for determining isotopic composition of elements by thermal ionization source mass spectrometry
Application to strontium

Giancarlo Cavazzini*

Laboratorio di Geocronologia, C.N.R. Istituto per le Geoscienze e le Georisorse, Corso Garibaldi 37, 35137 Padova, Italy

Abstract

It is shown that in thermal ionization source mass spectrometry, if isotope fractionation of the element in the sample follows a linear law, straight-line distributions in x_m versus x_m/y_m diagrams are observed, where x_m and y_m are two measured isotope ratios. The slopes and y-intercepts of these linear distributions are functions of the 'true' (starting) values x_t and y_t of the element in the sample and of the masses of the isotopes involved in ratios x and y. Since the masses of the nuclides are known, true ratios x_t and y_t can be calculated. This theoretical result is used to determine the non-radiogenic part of the isotopic composition of strontium in NBS SRM 987, one ^{84}Sr-enriched isotopic tracer prepared at the Oak Ridge National Laboratory, and two natural samples (rocks from the metamorphic basement of the Italian Eastern Alps) without any assumption about the isotopic composition itself.

Strontium was loaded as nitrate on single tungsten filaments, and ^{88}Sr/^{86}Sr and ^{84}Sr/^{86}Sr ratios were measured up to a fractionation of ~1% u^{-1} in a single-collector VG 54E mass spectrometer. For each run, ^{86}Sr/^{88}Sr, ^{84}Sr/^{86}Sr and ^{84}Sr/^{88}Sr ratios were calculated for all useful x_m versus x_m/y_m distributions. The respective weighted average values are considered the true values of the isotope ratios in the sample.

Four runs of isotopic standard NBS SRM 987 and one run of the isotopic tracer gave accurate and reproducible results which are identical, within error limits, to the respective certified values. The four determinations of NBS 987 resulted in the following weighted average values: ^{86}Sr/^{88}Sr = 0.11942 ± 0.00018; ^{84}Sr/^{86}Sr = 0.056485 ± 0.000075; ^{84}Sr/^{88}Sr = 0.006746 ± 0.000017 (error at 2σ level).

The values of the natural ^{86}Sr/^{88}Sr ratio (two rocks: 0.11956 ± 0.00017 and 0.11957 ± 0.00008; NBS 987: 0.11942 ± 0.00018) are identical within error limits, and identical or very close to the recommended value of 0.1194, the worldwide assumed 'true' ^{86}Sr/^{88}Sr value in the commonly used procedure of determining ^{87}Sr/^{86}Sr ratio by normalization.

However, due to the accuracy of the above determinations, it is suggested that, in nature, significant differences exist in the non-radiogenic part of the isotopic composition of strontium.
© 2004 Elsevier B.V. All rights reserved.

Keywords: Mass spectrometry; Thermal ionization; Isotope fractionation; Linear model; Isotope ratios

1. Introduction

Thermal ionization source mass spectrometry is widely used in Earth Sciences to determine the isotopic compositions of metals (for example, Sr, Nd, Pb, etc.) which are important in geological investigations, such as dating minerals and rocks and/or inferring information about the genesis and evolution of geological materials [1–3].

A fundamental problem in surface ionization source mass spectrometry is that the evaporation rates of the isotopes of the element of interest from the filament differ. This generates fractionation of the isotopes in the sample, and the measured values of isotope ratios which change in time [4,5]. For this reason, in Sr laboratory routines, measured ^{87}Sr/^{86}Sr ratios are corrected ('normalized') according to the instantaneous shifts of the measured ^{86}Sr/^{88}Sr ratio from a

* Tel.: +39 049 827 2002; fax: +39 049 827 2010.
E-mail addresses: Giancarlo.Cavazzini@igg.cnr.it,
gianca@dmp.unipd.it (G. Cavazzini).

value which is assumed to be 'true' for the sample (0.1194 [6–8]).

The normalization procedure implies assumptions about: (i) the isotopic composition of the element and (ii) the model according to which isotope fractionation occurs during the run. However, rigorous determination of the isotopic composition of an element in a sample should avoid assumptions, in particular, assumptions about the isotopic composition itself.

These assumptions are doubly dangerous. First, they prevent us from detecting if differences exist in some parts of the isotopic composition. Second, the values of the normalized ratio strongly depend on the 'true' reference values. In the case of Sr, a 0.1% deviation of the $^{86}Sr/^{88}Sr$ ratio from the ideal value of 0.1194 leads to a deviation of 0.04% of the corrected $^{87}Sr/^{86}Sr$ ratio (approximately three units on the fourth decimal digit), which is at least one order of magnitude higher than the typical error for $^{87}Sr/^{86}Sr$.

Assumptions about the isotopic compositions of the natural sample and the tracer are also often crucially used in isotope dilution schemes of calculations. In IDA, the accuracy and precision of results depend closely on knowledge of the isotopic composition of tracers. Hoffmann [9] proposed a method to determine tracer isotopic composition, which can be applied to elements composed of more than two isotopes. It consists of iterative mass spectrometer runs of the pure tracer and of a special natural-tracer mixture called 'critical' [9–12].

During the run of a critical mixture, the measured values of two isotope ratios x, y, with the same isotope at the denominator, define a fractionation straight line which coincides with the mixing straight line, obtained by plotting true (unfractionated) values of ratios x, y of natural-tracer mixtures. Therefore, the isotopic ratios x_s, y_s of the tracer are given by the intersection of the pure-spike fractionation line with the fractionation line defined by the critical mixture.

In Hoffmann's calculation, assumptions are made about the isotopic composition of strontium in the natural sample and in the tracer. These assumptions shed uncertainty on the calculated values of the isotope ratios. Moreover, we cannot neglect the fact that the very small angle which is defined by the pure-spike fractionation line and the natural-spike mixing line may greatly increase this uncertainty. The angle in question is approximately 0.2° for a ∼80% ^{84}Sr-enriched tracer, and becomes smaller and smaller as ^{84}Sr enrichment increases. It falls to 0.02° or less when the degree of enrichment is >98%, making determination of the isotopic composition of highly enriched strontium tracers by Hoffmann's method very problematic.

Assumptions about the law according to which isotope fractionation occurs during runs are also fundamental in normalizing data. In the literature, three models have been proposed, commonly known as 'Rayleigh's law', 'Power law' and 'Exponential law' [4,15–18]. A useful approximation, hereafter called 'linear model' of fractionation, has also been obtained by series-expanding the power law function and truncating the series to the first-order term [15–18].

The linear model was used worldwide in the 1960–1980s to correct measured isotope ratios for instrumental mass discrimination. It can still be validly used if fractionation is not large (approximately ≤0.5% u^{-1}) and within a certain range of fractionation [17,18]. For larger ranges (up to 1.7–1.8% u^{-1}), [17,18] showed that an exponential law model of fractionation ensures much better reductions of the observed data, so that for correcting measured isotopic ratios from instrumental mass discrimination, the linear model has progressively been abandoned. This useful approximations, however, is still conveniently used to describe instrumental isotope fractionation in IDA models of calculation [9,13,14,19].

This paper proposes a new method of analysis and calculation which represents an attempt at solving these problems. In the following, it is shown that the "true" (starting) isotope ratios of an element of interest in a sample can be determined by thermal ionization mass spectrometry virtually without any assumptions. This method can be applied to elements which are composed of more than two isotopes, and determination of part of the isotopic composition of strontium in isotopic standards and natural samples is illustrated.

2. Theory and calculation

2.1. Calculation of true isotope ratios

Briefly, the linear model assumes that, at any instant, the difference between measured and true (starting) values, per unit of measured value and per unit of mass difference between the two isotopes involved in the ratio, is the same for any isotope ratio of the element in question.

Calling the i/j isotope ratio x, we can write:

$$\frac{x_m - x_t}{x_m(M_j - M_i)} = F. \tag{1}$$

where F is the 'fractionation factor'; x_m, x_t, the instantaneously measured and starting (true) values of the isotope ratio, respectively; and M_i, M_j, the masses of isotopes i, j, respectively.

Following the basic hypothesis, for two different isotope ratios x and y, we can write:

$$\frac{x_m - x_t}{x_m \Delta M_x} = \frac{y_m - y_t}{y_m \Delta M_y} \tag{2}$$

where ΔM_x, ΔM_y are mass differences calculated between the isotope at the denominator and at the numerator in isotope ratios x, y, respectively.

Eq. (2) can be solved to yield y_m:

$$y_m = \frac{-x_m y_t \Delta M_x}{x_m(\Delta M_y - \Delta M_x) - x_t \Delta M_y}. \tag{3}$$

Clearly, the relationship between the two isotope ratios is not linear. Nevertheless, the relationship x_m versus x_m/y_m is

linear:

$$\frac{x_m}{y_m} = \left(\frac{x_t}{y_t}\right)\left(\frac{\Delta M_y}{\Delta M_x}\right) + x_m\left(\frac{\Delta M_x - \Delta M_y}{y_t \Delta M_x}\right) \quad (4)$$

Eq. (4) shows that the slope and y-intercept of the straight line depend on the true values of isotope ratios x_t, y_t and on mass differences ΔM_x, ΔM_y between the isotopes involved in the ratios. Since ΔM_x, ΔM_y are known to a certain degree of accuracy, slope and y-intercept are dependent only on true values x_t, y_t.

Thus, it is possible to calculate the true values of the isotope ratios of the element in the sample by straight-line best-fit of points in x_m versus x_m/y_m diagrams, i.e., from measured values only. We calculate y_t from value m of the slope of the best-fit:

$$y_t = \frac{1}{m}\frac{\Delta M_x - \Delta M_y}{\Delta M_x} \quad (5)$$

and x_t from slope m and value q of the y-intercept:

$$x_t = \frac{q}{m}\frac{\Delta M_x - \Delta M_y}{\Delta M_y} \quad (6)$$

This means that, if during a mass spectrometer run the process of isotope fractionation in the sample follows the linear model of fractionation, the isotope ratios of the element in the sample can be determined without any assumptions about the isotopic composition itself. However, the element must be composed of at least three isotopes, because two different ratios, x and y, are necessary for the calculations.

Fig. 1 shows one of the possible x_m versus x_m/y_m plots which can be drawn using data obtained for sample LASA 7 (a rock from the metamorphic basement of the Italian Eastern Alps). The good linear correlations shown by these x_m versus x_m/y_m distributions are interpreted as strontium in the
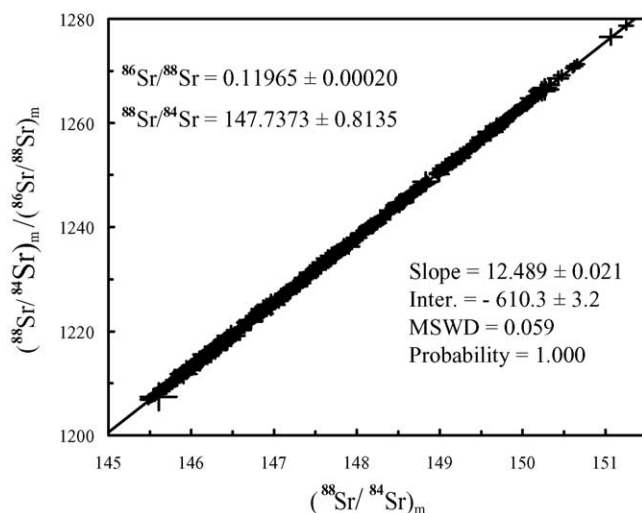

Fig. 1. $(^{88}Sr/^{84}Sr)_m$ vs. $(^{88}Sr/^{84}Sr)_m/(^{86}Sr/^{88}Sr)_m$ diagram for sample LASA 7. Also shown: straight-line best-fit parameters and calculated values of $(^{86}Sr/^{88}Sr)_t$ and $(^{88}Sr/^{84}Sr)_t$. Errors on best-fit parameters at 95% confidence level. Errors on calculated 'true' ratios by 2σ error propagation.

sample isotopically fractionated during the run according to a linear law. Thus, the $^{86}Sr/^{88}Sr$ and $^{88}Sr/^{84}Sr$ ratios in sample LASA 7 can be calculated from the linear best-fit parameters (slope = 12.489 ± 0.021; y-intercept = -610.3 ± 3.2) and from the values of the masses of the nuclides involved.

The accuracy and precision on the calculated values of x_t, y_t depend on the accuracy and precision of the slopes and y-intercepts, which result from straight-line best-fit calculations. Due to errors which afflict the measured ratios, the larger the interval of fractionation (i.e., the longer the straight-line segments), the more accurate m and q.

However, [17,18] showed that the linear law model of fractionation can successfully be used in data reduction only if the fractionation range is not large and only within a certain range of fractionation values. If fractionation is large, an exponential law model can be better applied. For this reason, it becomes particularly important to derive a linear approximation of the exponential model of fractionation.

By re-arranging Eqs. (1) and (3) in [18], the following condition for linear approximation of the exponential law can be written:

$$(x_m - x_t)/[x_m \cdot \ln(M_i/M_j)] = F \quad (7)$$

where $x = i/j$.

Thus, the equations, which calculate the true ratios, become:

$$y_t = (1/m)[1 - \ln(M_n/M_d)_y/\ln(M_n/M_d)_x] \quad (8)$$

and

$$x_t = (q/m)[\ln(M_n/M_d)_x/\ln(M_n/M_d)_y - 1] \quad (9)$$

where $(M_n/M_d)_x$ is the ratio between the mass of the isotope at the numerator (M_n) and that at the denominator (M_d) in ratio x.

We can obtain experimental evidence that the linear hypothesis is fulfilled if x_m and x_m/y_m are linearly correlated. If this is so, the values of the true isotope ratios of the element in the sample can be determined virtually without any assumptions.

In general, in a mass spectrometric run which collects the signals of three different isotopes of an element, the two measured isotope ratios, x_m and y_m, the ratio z_m, which can be calculated from their combination and their respective inverted ratios, can be used to draw 24 x_m versus x_m/y_m distributions. Each of these can be used to calculate one ratio x_t, one ratio y_t, and ratio z_t generated from the combination of the calculated values of x_t and y_t. In general, ratios x_t, y_t and z_t differ. For example, if the ^{84}Sr, ^{86}Sr and ^{88}Sr peaks are collected and the $^{88}Sr/^{86}Sr$ and $^{84}Sr/^{86}Sr$ ratios are measured, we can plot distribution $(^{84}Sr/^{86}Sr)_m$ versus $(^{84}Sr/^{86}Sr)_m/(^{88}Sr/^{84}Sr)_m$, distribution $(^{88}Sr/^{86}Sr)_m$ versus $(^{88}Sr/^{86}Sr)_m/(^{84}Sr/^{88}Sr)_m$, and many others. From the first distribution we calculate $x_t = {}^{84}Sr/^{86}Sr$, $y_t = {}^{88}Sr/^{84}Sr$ and $z_t = {}^{88}Sr/^{86}Sr$ (and the respective inverse ratios $1/x_t = {}^{86}Sr/^{84}Sr$, $1/y_t = {}^{84}Sr/^{88}Sr$ and $1/z_t = {}^{86}Sr/^{88}Sr$). From the second distribution, we calculate

$x_t = {}^{88}Sr/{}^{86}Sr$, $y_t = {}^{84}Sr/{}^{88}Sr$ and $z_t = {}^{84}Sr/{}^{86}Sr$ (and the respective inverse ratios $1/x_t = {}^{86}Sr/{}^{88}Sr$, $1/y_t = {}^{88}Sr/{}^{84}Sr$ and $1/z_t = {}^{86}Sr/{}^{84}Sr$) so that, in the end, we obtain 24 values for ${}^{86}Sr/{}^{88}Sr$, 24 for ${}^{84}Sr/{}^{86}Sr$, and 24 for ${}^{84}Sr/{}^{88}Sr$. These values should be, respectively, consistent within the error limits. If this condition is fulfilled, the values of these ratios can be used to calculate weighted averages which can be considered as the isotope ratios of the element in the sample. Fig. 2 shows the mutual consistency within error limits of the values of 'true' ${}^{86}Sr/{}^{88}Sr$ calculated from the x_m versus x_m/y_m distributions for sample NBS 987/3. From left to right, the $({}^{86}Sr/{}^{88}Sr)_t$ values are, respectively, obtained from the x_m versus x_m/y_m distributions as arranged, for example, in Table 4. It will be noted that only 20 (not 24) values are reported. This is due to collected peaks ${}^{84}Sr$, ${}^{86}Sr$ and ${}^{88}Sr$: in four x_m versus x_m/y_m plots $\Delta M_x \approx \Delta M_y$, so that the slopes of the distributions are very close to 0, whereas errors on x_m and x_m/y_m lead to unreliable x_t and y_t results. These results were not considered in the weighted average calculations.

2.2. Errors

Comparison of Eqs. (5) and (8) with (6) and (9) shows that the values of x_t, y_t and z_t calculated from different diagrams are afflicted by somewhat different errors. Whereas the only errors, which afflict the calculated value of y_t, are errors on slope m and the masses of the isotopes involved, the error which afflicts ratio x_t involves not only errors on slope m and masses, but also those on y-intercept q. And the largest error afflicts z_t, because this ratio is calculated by combining ratios x_t and y_t. Thus, the error which afflicts a certain $(i/j)_t$ ratio, calculated using a certain x_m versus x_m/y_m distribution, is different according to whether ratio $(i/j)_t$ is x, y or z in that diagram.
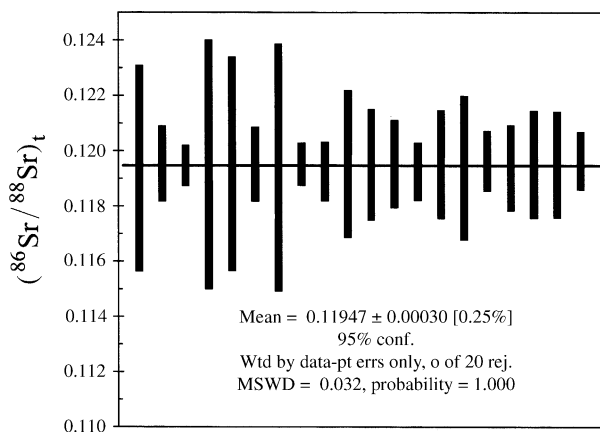
Fig. 2 shows that error bars of different sizes characterize the values of $({}^{86}Sr/{}^{88}Sr)_t$ calculated from different distributions.

The relative error which afflicts slope m can be shown to depend on the relative error which afflicts angle θ with the abscissa, according to the equation:

$$\frac{dm}{m} = M \left(\frac{d\theta}{\theta} \right) \tag{10}$$

where:

$$M = \frac{\theta}{\mathrm{sen}\theta\cos\theta} \tag{11}$$

is a magnification factor.

For positive slopes, $M < 2$ for angles less than $\sim55°$. Thereafter, it increases dramatically. On the other hand, $d\theta/\theta$ decreases with increasing θ, so that, as the slope increases, M and $d\theta/\theta$ tend to compensate. The accuracies of the values of the isotope ratios which are calculated from a certain x_m versus x_m/y_m distribution, therefore, depend mostly on the 'position' of the ratios in that distribution (ratio x on the abscissa, ratio y as the denominator on the ordinate, or ratio z as the combination of ratio x and ratio y).

3. Experimental

3.1. Sample preparations

The standard NBS SRM 987 ($SrCO_3$, alkalimetric assay; weight percent, 99.98 ± 0.02) was dissolved in 0.1N HNO_3 to give a solution of approximately 400 µg/ml. About 0.5 µl of the solution were loaded on a single tungsten filament over a small drop of a solution of $TaCl_5$ (the latter prepared by dissolving 2.4 g of Janssen Ta-V chloride in 1 ml ultrapure HF, 1 ml of 0.025 M H_3PO_4 and 18 ml of water).

First, the base drop of $TaCl_5$ solution was dried at a current of 0.3 A. Then, the sample solution was loaded on and dried at the same current value. Lastly, the filament was heated very slowly until it began to glow a very dull red (approximately 2.5 A current), which was held for approximately 5 s.

The amount of tracer (a Sr carbonate prepared at the Oak Ridge National Laboratory, U.S.A.) was dissolved in 2.5N HCl and water. About 1 ml of the solution (strontium concentration, $\sim1.16 \times 10^{-7}$ mol Sr/g) was evaporated to dryness. The residue was dissolved in 1.5 ml of 2.5N HCl, and ~0.3 ml of this solution were loaded above a column of cation-exchange resin (BioRad AG 50W x-12) and eluted with 2.5N HCl to separate rubidium from strontium. The Sr-containing solution was then evaporated to dryness and $SrCl_2$ was changed to $Sr(NO_3)_2$ by adding 2×0.1 ml of 10N HNO_3. After final evaporation to dryness, the sample was dissolved in 0.5N HNO_3, and approximately 0.4 µg of strontium were loaded on a single tungsten filament, following the procedure described for NBS 987.

Fig. 2. Weighted average of $({}^{86}Sr/{}^{88}Sr)_t$ values for sample NBS 987/3. From left to right: $({}^{86}Sr/{}^{88}Sr)_t$ values, respectively, calculated from x_m vs. x_m/y_m distributions, as listed in Table 4. First eight values (bars) result from unambiguous distributions, and next 12 from ambiguous ones. Error bars of different size characterize values of $({}^{86}Sr/{}^{88}Sr)_t$ calculated from different distributions, according to whether ratio ${}^{86}Sr/{}^{88}Sr$ represents ratio x, y or z in distribution.

Two rock samples, biotite and muscovite micaschists coming from the LASA Formation, a metamorphic unit of the crystalline basement of the Italian Eastern Alps, were finely ground and ~0.1 g of each sample were dissolved using concentrated HF and HNO_3 in a Savillex teflon vial. The sample dissolution procedure is described in detail in [23,24]. Approximately 0.3 ml of the final solution of the sample, in the form of 2.5N HCl, were loaded above a column of AG 50W x-12 BioRad cation-exchange resin, to separate Sr from Ca and Rb. The Sr-containing volume of eluant (~15 ml) was then evaporated to dryness and $SrCl_2$ was changed to $Sr(NO3)_2$ by adding 2 ml × 0.1 ml of ultrapure HNO_3. After final evaporation to dryness, the sample was dissolved in 0.5N HNO_3, and approximately 1–2 μg of strontium were loaded on a single tungsten filament, following the procedure described for NBS 987.

3.2. Mass spectrometry

The W single filaments (99.95% W; thickness, 0.001 in.; width, 0.020 in.) were degassed in a VG degassing unit under a pressure $<2.0 \times 10^{-5}$ mbar according to the following procedure: 10 min at 2.2 A and 30 min at 3.3 A.

A VG Micromass 54E single-collector mass spectrometer was used. Electromagnetic parameters and other approximate working conditions were: accelerating potential, 8 kV; approximate magnet current, 3.2 A; vacuum in the flight tube better than 3×10^{-8} mbar. The data acquisition program was [20].

Filament current was increased to 2.0 A at a rate of 1 mA/s. Thereafter, operating current values (in the range, 2.5–2.7 A) were reached at a slower rate (0.2 mA/s).

The non-radiogenic part of the isotopic composition of strontium was determined, i.e., the three peaks ^{84}Sr, ^{86}Sr and ^{88}Sr were sampled and the $^{84}Sr/^{86}Sr$ and $^{88}Sr/^{86}Sr$ ratios were measured. Integration times on peaks of 1 s and waiting times of 1 s were adopted.

Due to the very small intensity of the ^{84}Sr peak, it was necessary to maintain a high ^{88}Sr signal (>7 V, better >8–9 V) (^{84}Sr peak, ~55–65 mV) in order to reduce errors on the measured $^{84}Sr/^{86}Sr$ ratios. Small changes in the filament current were sometimes required to maintain the ^{88}Sr signal at >7 and <10 V, which is the maximum voltage permitted for reproducible behavior of the Faraday amplifier circuit.

Blocks of 30 ratios each were sampled. Depending on sample, approximately 150–1400 data blocks were acquired. Typical percent errors on the mean in a block were <0.06 and <0.03 for $^{84}Sr/^{86}Sr$ and $^{88}Sr/^{86}Sr$, respectively. Correction for resistor decay constants were 750–770 and 4800–5000 ppm ratio for $^{88}Sr/^{86}Sr$ and $^{84}Sr/^{86}Sr$, respectively.

Four determinations of $^{86}Sr/^{88}Sr$, $^{84}Sr/^{86}Sr$ and $^{84}Sr/^{88}Sr$ ratios were carried out for NBS 987, and single determinations for the Oak Ridge ^{84}Sr-enriched tracer and for rock samples LASA 4 and LASA 7. As regards natural strontium (NBS 987 and samples LASA 4 and LASA 7), runs of 1–6 days were necessary to cause a change in the $^{86}Sr/^{88}Sr$ ra-

tio from approximately 0.1205 to 0.1180 (a fractionation of ~1% u^{-1}, where u is the unit of mass difference) while the $^{84}Sr/^{86}Sr$ and $^{88}Sr/^{86}Sr$ ratios were continuously measured.

In the case of the isotopic tracer, the whole isotopic composition was determined by two separate runs. In the first run, which lasted approximately four days (940 continuously sampled blocks of data), the new method was applied and the $^{86}Sr/^{88}Sr$, $^{84}Sr/^{86}Sr$ and $^{84}Sr/^{88}Sr$ ratios were determined. The range of fractionation was approximately 0.8% u^{-1}. In the second run, for a more accurate result, the $^{87}Sr/^{86}Sr$ ratio was determined by normalizing the measured $^{87}Sr/^{86}Sr$ ratios to the average value of the $^{86}Sr/^{88}Sr$ ratio obtained in the first run. In this run, the ^{85}Rb peak was carefully monitored before and after each block of data, in order to quantify any interferences of the ^{87}Rb peak in the ^{87}Sr peak. ^{85}Rb intensity was about 0.2 mV, and the correction on the ^{87}Sr peak was between 0.06 and 0.07%.

4. Results and discussion

The values of the masses of strontium isotopes and the respective errors are from the Atomic Mass Data Center recommended files [21]. Statistics in [22] were used for straight-line best-fit calculations and weighted average calculations. Errors on best-fit slopes and y-intercepts are at 95% confidence level.

Errors on the isotopic ratios in Tables 1, 2, 4 and 5 and on the isotopic abundances in Table 3 were calculated by 2σ-error propagation.

The $^{86}Sr/^{88}Sr$ ratio in NBS 987 was originally determined by the Analytical Mass Spectrometry Group of the National Bureau of Standards by careful calibration for instrumental bias using samples of known $^{86}Sr/^{88}Sr$ ratios prepared from chemically pure and nearly isotopically pure ^{86}Sr and ^{88}Sr solutions [7]. The obtained value (0.11935 ± 0.00005) was then used to determine the value of the $^{84}Sr/^{86}Sr$ ratio by normalization (0.05655 ± 0.00014), assuming a linear law model for instrumental isotope fractionation. This strontium, of well-known isotopic composition was, therefore, ideal to test and calibrate the new method.

The results of four different runs of NBS 987 are shown in Table 1. Within error limits, the values of $^{86}Sr/^{88}Sr$, $^{84}Sr/^{86}Sr$ and $^{84}Sr/^{88}Sr$ are, respectively, identical and, in each case, they are identical to the certified values. Table 1 also lists, for each ratio, the weighted average of the four determinations. The values of $^{86}Sr/^{88}Sr$ (0.11942 ± 0.00018) and $^{84}Sr/^{86}Sr$ (0.056485 ± 0.000075) are in good agreement with the certified values.

The results of the determination of the isotopic composition of the tracer solution are shown in Tables 2 and 3. Table 2 lists the useful x_m versus x_m/y_m distributions and the respective calculated $^{86}Sr/^{88}Sr$, $^{84}Sr/^{86}Sr$ and $^{84}Sr/^{88}Sr$ values. It also shows, for each ratio, the weighted average value.

Table 3 compares the measured isotopic ratios and the calculated isotopic abundances with those reported on the cer-

Table 1
Measured isotopic ratios for NBS SRM 987

Sample	$^{86}Sr/^{88}Sr$	Error	$^{84}Sr/^{86}Sr$	Error	$^{84}Sr/^{88}Sr$	Error
NBS 987/1	0.11941	0.00053	0.05650	0.00023	0.006748	0.000026
NBS 987/2	0.11925	0.00048	0.05638	0.00020	0.006723	0.000024
NBS 987/3	0.11947	0.00030	0.05649	0.00012	0.006750	0.000015
NBS 987/4	0.11944	0.00030	0.05652	0.00013	0.006750	0.000015
Weighted averages	0.11942	0.00018	0.056485	0.000075	0.006746	0.000017

Results for NBS 987/1–NBS 987/4 are weighted averages (see Fig. 2). Also shown: weighted averages of results of the four determinations. All errors are at 95% confidence level.

Table 2
x_m vs. x_m/y_m distributions and respective $(^{86}Sr/^{88}Sr)_t$, $(^{84}Sr/^{86}Sr)_t$ and $(^{84}Sr/^{88}Sr)_t$ values for an ^{84}Sr-enriched tracer prepared at Oak Ridge National Laboratory (Tennessee, USA)

Diagram	$^{86}Sr/^{88}Sr$	Error	$^{84}Sr/^{86}Sr$	Error	$^{84}Sr/^{88}Sr$	Error
$(84/86)_m$ vs. $(84/86)_m/(88/84)_m$	0.29624	0.00275	22.501	0.150	6.666	0.017
$(88/86)_m$ vs. $(88/86)_m/(84/88)_m$	0.29632	0.00209	22.509	0.224	6.670	0.019
$(84/88)_m$ vs. $(84/88)_m/(88/86)_m$	0.29628	0.00080	22.504	0.309	6.668	0.073
$(84/88)_m$ vs. $(84/88)_m/(86/84)_m$	0.29695	0.00396	22.558	0.060	6.699	0.071
$(86/84)_m$ vs. $(86/84)_m/(84/88)_m$	0.29699	0.00278	22.561	0.151	6.700	0.018
$(86/88)_m$ vs. $(86/88)_m/(88/84)_m$	0.29688	0.00208	22.553	0.220	6.695	0.019
$(88/84)_m$ vs. $(88/84)_m/(84/86)_m$	0.29632	0.00397	22.505	0.061	6.669	0.071
$(88/84)_m$ vs. $(88/84)_m/(86/88)_m$	0.29693	0.00083	22.558	0.316	6.698	0.075
$(84/86)_m$ vs. $(84/86)_m/(88/86)_m$	0.29550	0.00076	22.442	0.179	6.632	0.070
$(84/86)_m$ vs. $(84/86)_m/(84/88)_m$	0.29760	0.00267	22.611	0.122	6.729	0.024
$(88/86)_m$ vs. $(88/86)_m/(84/86)_m$	0.29574	0.00243	22.463	0.062	6.643	0.073
$(88/86)_m$ vs. $(88/86)_m/(88/84)_m$	0.29763	0.00162	22.610	0.205	6.730	0.024
$(84/88)_m$ vs. $(84/88)_m/(86/88)_m$	0.29550	0.00078	22.444	0.179	6.632	0.035
$(84/88)_m$ vs. $(84/88)_m/(84/86)_m$	0.29748	0.00243	22.599	0.062	6.723	0.036
$(86/84)_m$ vs. $(86/84)_m/(88/84)_m$	0.29561	0.00260	22.451	0.118	6.637	0.024
$(86/84)_m$ vs. $(86/84)_m/(86/88)_m$	0.29773	0.00081	22.619	0.183	6.734	0.073
$(86/88)_m$ vs. $(86/88)_m/(84/88)_m$	0.29560	0.00158	22.453	0.200	6.637	0.024
$(86/88)_m$ vs. $(86/88)_m/(86/84)_m$	0.29748	0.00249	22.599	0.064	6.723	0.075
$(88/84)_m$ vs. $(88/84)_m/(86/84)_m$	0.29574	0.00245	22.462	0.063	6.643	0.036
$(88/84)_m$ vs. $(88/84)_m/(88/86)_m$	0.29774	0.00079	22.619	0.182	6.735	0.036
Weighted averages	0.29659	0.00044	22.530	0.029	6.682	0.016

Weighted averages are shown. All errors are at 95% confidence level.

Table 3
Certified and measured isotopic ratios and abundances for an ^{84}Sr-enriched tracer prepared at Oak Ridge National Laboratory (Table 2)

Certified ratios	$^{86}Sr/^{88}Sr$	Error	$^{84}Sr/^{86}Sr$	Error	$^{84}Sr/^{88}Sr$	Error	$^{87}Sr/^{86}Sr$	Error
	0.3020	0.0029	22.368	0.276	6.754	0.105	0.4201	0.0079
Certified abundances (%)	^{84}Sr	Error	^{86}Sr	Error	^{87}Sr	Error	^{88}Sr	Error
	82.54	0.10	3.69	0.05	1.55	0.05	12.22	0.05
Measured ratios	$^{86}Sr/^{88}Sr$	Error	$^{84}Sr/^{86}Sr$	Error	$^{84}Sr/^{88}Sr$	Error	$^{87}Sr/^{86}Sr$	Error
	0.29659	0.00044	22.530	0.029	6.682	0.016	0.422650	0.000019
Abundances (%)	^{84}Sr	Error	^{86}Sr	Error	^{87}Sr	Error	^{88}Sr	Error
	82.46	0.22	3.660	0.005	1.547	0.002	12.339	0.034

Errors on measured abundances calculated by 2σ-error propagation. Errors on certified ratios result from propagation of certified uncertainties on abundances.

tificate sheet. It is easily seen that the $^{84}Sr/^{86}Sr$ and $^{86}Sr/^{88}Sr$ ratios of the tracer solution are determined with much higher precision than that reported in the certificate of analysis. When compared with the critical-mixture method [9], this new method results in more accurate values of the isotopic ratios, while implying no assumptions (the only assumption is fulfilment of hypothesis (7), which is checked) and far less analytical work. The latter advantage cannot be neglected,

because any analytical work in itself represents an additional source of error.

Tables 4 and 5 list the useful x_m versus x_m/y_m distributions and the respective calculated $^{86}Sr/^{88}Sr$, $^{84}Sr/^{86}Sr$ and $^{84}Sr/^{88}Sr$ values for samples LASA 4 and LASA 7, respectively. They also show, for each ratio, the weighted average value. It can be seen that LASA 4 and LASA 7 have identical isotope ratio values. This was expected, because these sam-

Table 4

x_m vs. x_m/y_m distributions and respective $(^{86}Sr/^{88}Sr)_t$, $(^{84}Sr/^{86}Sr)_t$ and $(^{88}Sr/^{84}Sr)_t$ values for rock sample LASA 4

Diagram	$^{86}Sr/^{88}Sr$	Error	$^{84}Sr/^{86}Sr$	Error	$^{84}Sr/^{88}Sr$	Error
$(84/86)_m$ vs. $(84/86)_m/(88/84)_m$	0.11941	0.00226	0.05644	0.00076	0.006739	0.000037
$(88/86)_m$ vs. $(88/86)_m/(84/88)_m$	0.11951	0.00079	0.05648	0.00053	0.006750	0.000018
$(84/88)_m$ vs. $(84/88)_m/(88/86)_m$	0.11946	0.00043	0.05647	0.00103	0.006746	0.000099
$(84/88)_m$ vs. $(84/88)_m/(86/84)_m$	0.11962	0.00258	0.05657	0.00025	0.006767	0.000117
$(86/84)_m$ vs. $(86/84)_m/(84/88)_m$	0.11971	0.00220	0.05659	0.00075	0.006774	0.000035
$(86/88)_m$ vs. $(86/88)_m/(88/84)_m$	0.11963	0.00078	0.05655	0.00052	0.006765	0.000018
$(88/84)_m$ vs. $(88/84)_m/(84/86)_m$	0.11946	0.00251	0.05646	0.00023	0.006745	0.000114
$(88/84)_m$ vs. $(88/84)_m/(86/88)_m$	0.11966	0.00043	0.05656	0.00103	0.006768	0.000099
$(84/86)_m$ vs. $(84/86)_m/(88/86)_m$	0.11915	0.00061	0.05632	0.00086	0.006710	0.000137
$(84/86)_m$ vs. $(84/86)_m/(84/88)_m$	0.11979	0.00156	0.05663	0.00044	0.006784	0.000035
$(88/86)_m$ vs. $(88/86)_m/(84/86)_m$	0.11937	0.00110	0.05642	0.00017	0.006735	0.000083
$(88/86)_m$ vs. $(88/86)_m/(88/84)_m$	0.11978	0.00093	0.05663	0.00074	0.006783	0.000035
$(84/88)_m$ vs. $(84/88)_m/(86/88)_m$	0.11914	0.00059	0.05632	0.00084	0.006709	0.000067
$(84/88)_m$ vs. $(84/88)_m/(84/86)_m$	0.11976	0.00110	0.05662	0.00018	0.006780	0.000041
$(86/84)_m$ vs. $(86/84)_m/(88/84)_m$	0.11932	0.00154	0.05640	0.00044	0.006729	0.000035
$(86/84)_m$ vs. $(86/84)_m/(86/88)_m$	0.11996	0.00060	0.05671	0.00088	0.006803	0.000140
$(86/88)_m$ vs. $(86/88)_m/(84/88)_m$	0.11931	0.00094	0.05640	0.00074	0.006729	0.000035
$(86/88)_m$ vs. $(86/88)_m/(86/84)_m$	0.11977	0.00110	0.05661	0.00018	0.006780	0.000084
$(88/84)_m$ vs. $(88/84)_m/(86/84)_m$	0.11936	0.00111	0.05642	0.00018	0.006735	0.000042
$(88/84)_m$ vs. $(88/84)_m/(88/86)_m$	0.11996	0.00059	0.05671	0.00085	0.006803	0.000069
Weighted averages	0.11956	0.00017	0.056515	0.000070	0.0067571	0.0000085

Weighted averages are shown. All errors are at 95% confidence level.

Table 5

x_m vs. x_m/y_m distributions and respective $(^{86}Sr/^{88}Sr)_t$, $(^{84}Sr/^{86}Sr)_t$ and $(^{88}Sr/^{84}Sr)_t$ values for rock sample LASA 7

Diagram	$^{86}Sr/^{88}Sr$	Error	$^{84}Sr/^{86}Sr$	Error	$^{84}Sr/^{88}Sr$	Error
$(84/86)_m$ vs. $(84/86)_m/(88/84)_m$	0.11948	0.00111	0.05649	0.00037	0.006749	0.000018
$(88/86)_m$ vs. $(88/86)_m/(84/88)_m$	0.11949	0.00036	0.05649	0.00024	0.006751	0.000008
$(84/88)_m$ vs. $(84/88)_m/(88/86)_m$	0.11948	0.00021	0.05649	0.00049	0.006750	0.000047
$(84/88)_m$ vs. $(84/88)_m/(86/84)_m$	0.11964	0.00125	0.05657	0.00012	0.006768	0.000056
$(86/84)_m$ vs. $(86/84)_m/(84/88)_m$	0.11965	0.00114	0.05658	0.00038	0.006769	0.000018
$(86/88)_m$ vs. $(86/88)_m/(88/84)_m$	0.11963	0.00035	0.05657	0.00023	0.006767	0.000008
$(88/84)_m$ vs. $(88/84)_m/(84/86)_m$	0.11949	0.00125	0.05649	0.00012	0.006750	0.000056
$(88/84)_m$ vs. $(88/84)_m/(86/88)_m$	0.11965	0.00020	0.05657	0.00049	0.006769	0.000047
$(84/86)_m$ vs. $(84/86)_m/(88/86)_m$	0.11932	0.00030	0.05640	0.00043	0.006730	0.000068
$(84/86)_m$ vs. $(84/86)_m/(84/88)_m$	0.11974	0.00074	0.05662	0.00021	0.006780	0.000017
$(88/86)_m$ vs. $(88/86)_m/(84/86)_m$	0.11936	0.00051	0.05643	0.00008	0.006736	0.000039
$(88/86)_m$ vs. $(88/86)_m/(88/84)_m$	0.11974	0.00044	0.05662	0.00035	0.006779	0.000017
$(84/88)_m$ vs. $(84/88)_m/(86/88)_m$	0.11931	0.00031	0.05641	0.00044	0.006730	0.000035
$(84/88)_m$ vs. $(84/88)_m/(84/86)_m$	0.11977	0.00053	0.05663	0.00008	0.006782	0.000020
$(86/84)_m$ vs. $(86/84)_m/(88/84)_m$	0.11939	0.00073	0.05645	0.00021	0.006739	0.000016
$(86/84)_m$ vs. $(86/84)_m/(86/88)_m$	0.11982	0.00030	0.05665	0.00043	0.006788	0.000068
$(86/88)_m$ vs. $(86/88)_m/(84/88)_m$	0.11939	0.00045	0.05644	0.00035	0.006739	0.000017
$(86/88)_m$ vs. $(86/88)_m/(86/84)_m$	0.11977	0.00052	0.05663	0.00008	0.006782	0.000040
$(88/84)_m$ vs. $(88/84)_m/(86/84)_m$	0.11936	0.00051	0.05643	0.00008	0.006736	0.000019
$(88/84)_m$ vs. $(88/84)_m/(88/86)_m$	0.11982	0.00030	0.05665	0.00043	0.006788	0.000035
Weighted averages	0.119568	0.000083	0.056528	0.000042	0.0067589	0.0000072

Weighted averages are shown. All errors are at 95% confidence level.

ples come from the same metamorphic unit and were sampled not far from each other, so that they substantially represent sampling of the same rock.

4.1. Comparisons between linear model from power law and linear model from exponential law

The linear approximation of the exponential model of fractionation (7) was considered as the basic hypothesis for all calculations, because isotope fractionation did not follow the linear model (1). This can be checked if two ratios are considered, in which the mass difference between the isotopes involved is the same (for example, $^{86}Sr/^{88}Sr$ and $^{84}Sr/^{86}Sr$). In this case, if linear model (1) of fractionation is followed, the ratios between the instantaneously measured isotope ratios and the respective 'true' values define a linear distribution during the run [17]. The slope of the correlation is 1, and is independent of the values of the 'true' ratios [17].

Instead, severe deviations from this ideal behavior (2.5–3.0%) were observed. They can be interpreted as due to the dependence of the fractionation factor on mass-a dependence which is typical of isotope fractionation which follows an exponential law.

This is reflected by the degree of (respective) mutual consistency of the values of the $^{86}Sr/^{88}Sr$, $^{84}Sr/^{86}Sr$ and $^{84}Sr/^{88}Sr$ ratios which are calculated from the different x_m versus x_m/y_m distributions. Although the mean values of the weighted averages of $^{86}Sr/^{88}Sr$, $^{84}Sr/^{86}Sr$ and $^{84}Sr/^{88}Sr$ calculated using the linear model (1) are identical to the respective values calculated using the linear model proposed here (7), in all cases the above values calculated for the different distributions are, respectively, much more mutually consistent when model (7) is adopted, and a large decrease in MSWD values is observed, with a large increase in the probability of the final weighted average values. This confirms that linear approximation of the exponential model of fractionation fits the measured values of the isotopic ratios much better than linear approximation of the power law of fractionation.

4.2. 'Ambiguous' x_m versus x_m/y_m distributions

Since three peaks were collected and the measured isotopic ratios involve a common isotope (^{86}Sr), 12 of the distributions which are useful for calculations satisfy condition $x_m/y_m = z_m$, i.e., both Eq. (3) (which is not linear) and Eq. (4) (which is linear). For this reason, we call them 'ambiguous'.

The doubtful character of these distributions seems to be reflected in the MSWD and fitting probability values yielded obtained by the linear best-fit calculations. For some of these distributions, the MSWD values are high (1.2–1.7) and the probability of linear fitting is 0. In other cases, the MSWD values are higher and the probability values are (sometimes) lower than for the unambiguous distributions (in the range 0.94–1.1 and 0.2–1, respectively) to indicate that, if linear, these distributions are 'less linear' than the unambiguous ones. Lastly, in yet other cases, the MSWD values are comparable to those obtained for some unambiguous distributions and fitting probability is 1, indicating that the distributions are linear as the unambiguous ones.

The values of $^{86}Sr/^{88}Sr$, $^{84}Sr/^{86}Sr$ and $^{84}Sr/^{88}Sr$ calculated from the unambiguous distributions ($x_m/y_m \neq z_m$) are, respectively, always mutually consistent, i.e., all of them are identical within respective error limits. The same is observed for $^{86}Sr/^{88}Sr$, $^{84}Sr/^{86}Sr$ and $^{84}Sr/^{88}Sr$ values obtained from ambiguous diagrams, but not always.

Nevertheless, for each sample, the mean values of the weighted averages of $^{86}Sr/^{88}Sr$, $^{84}Sr/^{86}Sr$ and $^{84}Sr/^{88}Sr$ calculated from the 12 ambiguous diagrams are always identical, respectively, to the mean values of the weighted averages calculated from the 8 unambiguous ones. For this reason, and for this may contribute to reduce errors, in this work all the distributions are used together to calculate global weighted averages of $^{86}Sr/^{88}Sr$, $^{84}Sr/^{86}Sr$ and $^{84}Sr/^{88}Sr$.

Fig. 2 shows the $^{86}Sr/^{88}Sr$ values calculated from all the useful distributions for sample NBS 987/3. From left to right, the first 8 values (bars) result from unambiguous distributions and the other 12 from ambiguous ones.

4.3. Drifting of average values of isotope ratios

Let us now consider one of the useful (x_m, x_m/y_m) distributions. The values of $^{86}Sr/^{88}Sr$, $^{84}Sr/^{86}Sr$ and $^{84}Sr/^{88}Sr$ can either be calculated over the whole data set, i.e., the whole recorded fractionation range ($\sim1\%$ u^{-1}), or from only parts of it: for example, the part up to fractionation is approximately 0.5% u^{-1} from the beginning of data acquisition. The means of the calculated values are seen to change, in particular, they slowly but progressivley drift as the fractionation range becomes larger (i.e., as the line segment becomes longer).

This drift is due to gradual changes in the best-fit parameters, which is evidence that the observed x_m versus x_m/y_m distributions are not perfectly linear. The relative changes in the best-fit slopes fall roughly in the range 0.7–2.4%.

Drifting of the mean values of the $^{86}Sr/^{88}Sr$, $^{84}Sr/^{86}Sr$ and $^{84}Sr/^{88}Sr$ ratios calculated for each x_m versus x_m/y_m distribution also causes the respective mean values of the weighted averages to drift. Fig. 3 shows the weighted average change of the $^{86}Sr/^{88}Sr$ values for sample NBS 987/3 with increasing fractionation. The amount of drift can be estimated by linear best-fit interpolation to the y-axis. In Fig. 3, the value of the y-intercept is 0.12039, so that drifting of the mean value is approximately 0.76% (i.e., 0.38% u^{-1}) for fractionation of 1% u^{-1}.

For proper data comparison, drifting cannot be neglected. This problem can be reduced or avoided by acquiring the data within the same interval of fractionation values. In the case of natural strontium, and in terms of $^{86}Sr/^{88}Sr$, the range of fractionation from approximately 0.1205 to 0.1180 was
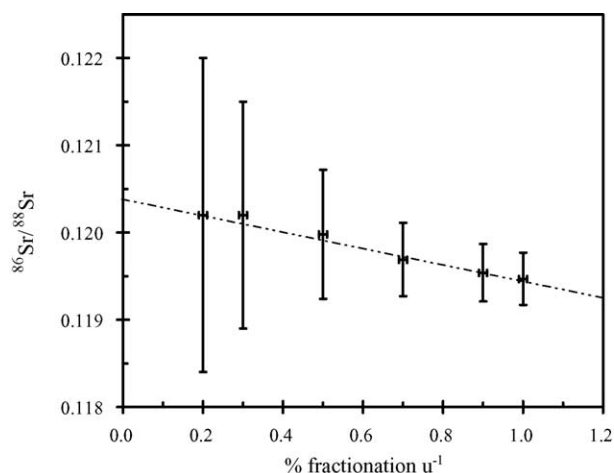

Fig. 3. Drift of weighted average of ($^{86}Sr/^{88}Sr$)$_t$ values with increasing fractionation for sample NBS 987/3. Estimated drift of mean value is approximately 0.38% u^{-1} for fractionation of 1% u^{-1}. Error bars on x are merely indicative; error bars on y represent $\pm2\sigma$.

chosen (a change of $\sim$1% u^{-1}), because: (i) it is sufficiently large to ensure sufficient precision of the calculated x_t and y_t values; (ii) it can quite easily be covered during analysis of most natural samples using standard laboratory routines; (iii) it ensures 'true' x_t and y_t values which can more confidently be used as normalization values for measurements of the ^{87}Sr/^{86}Sr ratio.

4.4. Changes in the non-radiogenic part of the isotopic composition of strontium

The values of the natural ^{86}Sr/^{88}Sr ratio (two rocks: 0.11956 ± 0.00017 and 0.11957 ± 0.00008; NBS 987: 0.11942 ± 0.00018) are identical within error limits, and identical or very close to the recommended value of 0.1194, which is the worldwide assumed 'true' ^{86}Sr/^{88}Sr value in the commonly used procedure of determining ^{87}Sr/^{86}Sr ratio by normalization.

However, since the above determinations are sufficiently accurate, it is likely that differences in the mean values of the ratios mostly reflect effective differences in the values of the isotope ratios themselves.

The accuracy of these determinations is indicated by the good match of the mean values of the ^{86}Sr/^{88}Sr and ^{84}Sr/^{86}Sr ratios measured for NBS 987 with the respective certified values, and by the match of the mean values of ^{86}Sr/^{88}Sr, ^{84}Sr/^{86}Sr and ^{84}Sr/^{88}Sr obtained from the two rock samples LASA 4 and LASA 7 (which substantially represent sampling of the same rock) since, with increasing accuracy, the mean values of the isotope ratios resulting from different determinations of the same sample must tend to coincide.

If this line of reasoning is correct, the ^{86}Sr/^{88}Sr and ^{84}Sr/^{88}Sr ratios in NBS 987 and LASA 4 and LASA 7 differ by about 0.12 and 0.20%, respectively.

It is striking that the calculated relative change in ^{84}Sr/^{88}Sr is approximately increased by a factor of 2 with respect to the relative change in ^{86}Sr/^{88}Sr. This is consistent with the strontium in NBS 987 being isotopically fractionated by mass-dependent processes with respect to the strontium in samples LASA 4/7 [25].

Further studies are obviously required in order to substantiate the hypothesis that strontium isotopes are fractionated in nature by mass-dependent processes.

5. Conclusions

At present, in thermal ionization source mass spectrometry, due to instrumental mass fractionation, the isotopic composition of strontium is measured by imposing a constraint on the isotopic composition itself $-^{86}$Sr/^{88}Sr $= 0.1194$ [6–8] – and the measured ^{84}Sr/^{86}Sr and ^{87}Sr/^{86}Sr ratios are "normalized" by calculating the shift of measured ^{86}Sr/^{88}Sr values from this recommended value. In this sense, normalizing data implies assumptions. Besides being philosophically in-

correct, the procedure is also limiting and dangerous. It is limiting because normalizing data to ^{86}Sr/^{88}Sr $= 0.1194$ makes it substantially impossible to ascertain whether differences in ^{86}Sr/^{88}Sr (and/or in other ratios of the non-radiogenic part of strontium isotopic composition) exist in nature. It is dangerous because it can give correct ^{87}Sr/^{86}Sr values only if the normalization value (0.1194) is correct for the sample.

In this paper, it is shown that possibilities do exist to measure the isotopic composition of strontium (and possibly of other elements) by thermal ionization source mass spectrometry without any assumptions about the isotopic composition itself. If isotope fractionation of the element in the sample follows a linear model, straight-line distributions in x_m versus x_m/y_m diagrams are observed, in which x_m and y_m are two measured isotope ratios. The slopes and y-intercepts of these linear distributions are functions of the 'true' (starting) values x_t and y_t of the element in the sample and of the masses of the isotopes involved in ratios x and y. Since these masses are known to a certain degree of accuracy, the true ratios x_t and y_t can be calculated. This method can be applied to elements with more than two isotopes.

Application to the determination of the non-radiogenic part of the isotopic composition of strontium in standard and natural samples is demonstrated here to give accurate and reproducible results. The values of natural ^{86}Sr/^{88}Sr ratio (two rocks: 0.11956 ± 0.00017 and 0.11957 ± 0.00008; NBS 987: 0.11942 ± 0.00018) are identical within error limits, and identical or very close to the recommended value of 0.1194, which is the worldwide assumed 'true' ^{86}Sr/^{88}Sr value in the commonly used procedure of determining ^{87}Sr/^{86}Sr ratio by normalization.

However, due to the accuracy of the above determinations, it is suggested that the observed differences in the mean values of the ratios reflect effective differences in the values of the isotope ratios themselves.

If this is correct, the natural ^{86}Sr/^{88}Sr and ^{84}Sr/^{88}Sr ratios differ by $\sim$0.12 and 0.20%, respectively. Similar differences cannot be ignored by the scientific community using TIMS, not only for correct determination of the ^{87}Sr/^{86}Sr ratio by normalization, but also for they represent new important information.

References

[1] G. Faure, Principles of Isotope Geology, second ed., John Wiley and Sons, New York, 1986.

[2] G. Faure, J.L. Powell, Strontium Isotope Geology, Springer-Verlag, Berlin, 1972.

[3] G. Faure, Origin of igneous rocks: the isotopic evidence, Springer, Berlin, 2001.

[4] A. Eberhardt, R. Delwiche, J. Geiss, Z. Naturforschg. 19a (1964) 736.

[5] C.E. Rees, Int. J. Mass Spectrom. Ion Phys. 3 (1969) 71.

[6] A.O. Nier, Physical Rev. 5 (1938) 275.

[7] L.J. Moore, T.J. Murphy, I.L. Barnes, P.J. Paulsen, J. Res. Natl. Bur. Stand. 87 (1982) 1.

[8] R.H. Steiger, E. Jager, Earth Planet. Sci. Lett. 36 (1977) 359.

[9] A. Hofmann, Earth Planet. Sci. Lett. 10 (1971) 397.

[10] L.E. Long, Trans. Am. Geophys. Union 46 (1965) 172.

[11] L.E. Long, Earth Planet. Sci. Lett. 1 (1966) 289.

[12] T.E. Krogh, P.M. Hurley, J. Geophys. Res. 73 (1968) 7107.

[13] J.C. Roddick, R.W. Sullivan, F.Ö. Dudás, Chem. Geol. 97 (1992) 1.

[14] R.W. Sullivan, J.C. Roddick, Geol. Surv. Can. Pap. 91–92 (1992) 201.

[15] M.H. Dodson, J. Sci. Instrum. 40 (1963) 289.

[16] M.H. Dodson, Geochim. Cosmochim. Acta 34 (1970) 1241.

[17] W.A. Russel, D.A. Papanastassiou, T.A. Tombrello, Geochim. Cosmochim. Acta 42 (1978) 1075.

[18] S.R. Hart, A. Zindler, Int. J. Mass Spectrom. Ion Process. 89 (1989) 287.

[19] W. Compston, V.M. Oversby, J. Geophys. Res. 74 (1969) 4338.

[20] K.R. Ludwig, U.S. Geol. Surv. Open File Rep. 92–543 (1993) 1.

[21] G. Audi, A.H. Wasptra, Nucl. Phys. A595 (1995) 409.

[22] K.R. Ludwig, Berkeley Geochronol. Center Special Pub. 4 (2003) 1.

[23] P.J. Potts, Handbook of Silicate Rock Analysys, Blackie, London, 1987.

[24] J. Blichert-Toft, IPGP Int. Rep. (1994) 1.

[25] H.C. Urey, J. Chem. Soc. (1947) 562.